Periodico di Mineralogia (2013), 82, 3, 477-487 DOI: 10.2451/2013PM0028

PERIODICO di MINERALOGIA
established in 1930

An International Journal of
MINERALOGY, CRYSTALLOGRAPHY, GEOCHEMISTRY,
ORE DEPOSITS, PETROLOGY, VOLCANOLOGY
and applied topics on *Environment*, *Archeometry* and *Cultural Heritage*

Scientific analyses beyond the excavation: studies for a non invasive preliminary approach

Letizia Bonizzoni[1,*], Valentina Brunello[1] and Simone Caglio[2]

[1] Dipartimento di Fisica, Università degli Studi di Milano, Via Celoria 16, Milano, Italy
[2] Freelance researcher, Via Matteotti 28, Carate Brianza (MB), Italy
[*]Corresponding author: *letizia.bonizzoni@mi.infn.it*

Abstract

Domo is an archaeological site located in the Foreste Casentinesi National Park, near the town of Bibbiena, in the province of Arezzo (Tuscany). Since the '80, investigations at Domo have revealed a Roman domus with a Roman baths complex. Unfortunately, the rich stratigraphy was almost completely lost during the first excavations. Since 2008 the archaeological site was reopened by Archeodomani s.a.s., a company that deals with promotion of cultural heritage, and it is still under summer excavation campaigns. In the future perspective to try and solve doubts about the site phase sequence of the Roman baths complex, not easy to understand now for several use modifications of the different areas, we developed an analytical method that could allow a large scale investigation limiting the sampling. In this paper, the preliminary results obtained for mortar are presented, both from the walls and from the binding of cocciopesto of the floor, with XRD (X Ray Diffraction) and ED-XRF (Energy Dispersive X-Ray Fluorescence) analysis on ground samples. XRD analysis was performed at ICVBC-CNR (Milan) and the diffraction data (Cu-Ka, 1.5418 Å) were collected on a J-J Panalytical X'Pert PRO diffractometer. Grounded samples were placed in aluminium sample holder or dusted on frosted glass sample holder, depending on sample amount. XRF measurements were performed at Physics Department of Milan University using a portable EDXRF spectrometer (Assing Lithos 3000) exploiting polychromatic radiation from a Mo anode X-ray tube. Both analyses were performed after preliminary observation of the samples by stereo-microscope and the results obtained through XRF and XRD analyses were compared to get more complete information about samples. Data were also submitted to multivariate analysis (Hierarchical Clustering) to get material classification. The comparison between the classification obtained and archaeological interpretation is still in progress; the collection of analytical data will go on in future excavation campaigns. The complete overview will be part of a project to promote the archaeological site through an online portal.

Key words: Mortar; XRD; ED-XRF; archaeology; multivariate analysis; in situ analysis.

Introduction

Mortars are materials resulting of the combination of sand grains, a binder (for instance: lime, cement...) and water. Their characteristics depend on the nature of the binder component. In the same way, historic mortars are made of combinations at different proportions of aggregates, binder and eventually some additives, too; with the consolidation of the Roman civilization, the use of lime mortars was generalized and extended (Adam, 1989). The aggregates are siliceous and carbonate from rivers or crushed rock. Thus, the production of mortars depended on the availability of raw materials and hence the mineralogical composition is especially relevant to establish direct correlation between provenance and use. Moreover, the use of specific materials reflects the technological capabilities and developments of the society. Many analytical techniques are generally employed, each with particular strengths and limitations; it is evident that combining together more of them, better results are achieved. Excluding photography and visual inspections, sampling is always required for mortar analyses, such as microscopy and thin section observation, scanning electron microscope, gas chromatography, thermal analysis and some others. Among these, XRD analysis plays a fundamental role, sometimes in association with elemental chemical characterization, for its ability to recognize mineralogical phases leaving samples undamaged for further investigations. Along with XRD and several other analytical techniques, ED-XRF analysis is often applied to get provenance classification of ceramics (Tite, 2008) on the bases of minor and trace elements. Moreover, the new generation of portable spectrometers allows a rapid and easy scan of large areas even if energy is not provided in situ.

In this work, ED-XRF measurements were performed to obtain the elemental composition of the mortars and to attempt a classification of the samples through HCA (hierarchical clusters analysis), comparing results with XRD based classification, more widely used. This would allow, for the future, to perform large scales investigations with portable XRF spectrometers, recognizing different typology of materials. Then, on the bases of the obtained results, sampling could be done according to recognized groups to deeper investigate the material morphology and mineralogical composition.

The archaeological site of Domo, in the Foreste Casentinesi National Park, near the town of Bibbiena, in the province of Arezzo (Tuscany), come up to be suitable for testing this methodology (Aranguren, 1999). In fact, its rich stratigraphy was almost completely lost during the first excavations in the 80's and the final aim of the research is to try and solve doubts about the site phase sequence of the Roman baths complex, not easy to understand now for several use modifications of the different areas. Here preliminary studies are presented, about the possibilities to discriminate mortars species - but not only - in situ with portable instrument so as to be able to perform a limited number of targeted samples.

Methodological approach

In this paper, the preliminary results on a set of 33 samples of masonry mortars, collected in the site of Domo, are presented and discussed. Several Stratigraphic Units (SU) and different rooms of the domus were concerned, contemplating areas supposed of different building periods. In Table 1, all the samples are reported, together with a brief description. In Figure 1 the scheme of the samplings is shown.

Non-destructive ED-XRF analysis has been performed on ground samples with a portable spectrometer (Assing Lithos 3000) equipped with a low power X-ray tube with Mo anode and a Peltier cooled Si-PIN detector. The irradiated area on the sample was about 3.7 mm^2; the

Table 1. List and description of samples considered in this work.

SAMPLE	LOCATION AND DESCRIPTION
M82	Bed mortar collected from SU 82, wall NNE-SSW (Small Bath)
M151	Bed mortar from SU 151, wall NNE-SSW (Small Bath)
M21	Mortar from the cocciopesto’s floor from SU 21 (Small Bath)
M5	Bed mortar from SU 5. Collected from the wall of the SU 5 (Small Bath)
M3	Bed mortar from SU 3. Collected from the wall of the SU 3 (Small Bath)
M177C_b	Bed mortar from SU 177, external wall, side W (Big Bath Tepidarium)
M177C_g	Bed mortar from SU 177, external wall, side W (Big Bath Tepidarium)
M177A_g	Bed mortar from SU 177, external wall, side W (Big Bath Tepidarium)
M177A_b	Bed mortar from SU 177, external wall, side W (Big Bath Tepidarium)
M150C_g	Bed mortar from SU 150, Hypocaustum (Big Bath)
M150C_b	Malta (grumo) from SU 150, Hypocaustum (Big Bath Tepidarium)
M150A	Bed mortar from SU 150, Hypocaustum (Big Bath)
M150B_g	Bed mortar from SU 150, Hypocaustum (Big Bath)
M150B_b	Malta (lump) from SU 150, Hypocaustum (Big Bath)
M178B	Bed mortar from SU 178, external wall, side E (Big Bath)
M173A_b	Bed mortar (lump) from SU 173, wall WWN-ESE (Big Bath)
M173A_g	Bed mortar from SU 173, wall WWN-ESE (Big Bath)
M173C_g	Bed mortar from SU 173, wall WWN-ESE (Big Bath)
M173C_b	Bed mortar (lump) from SU 173, wall WWN-ESE (Big Bath)
M170B_g	Bed mortar from SU 170 (Big Bath)
M170B_b	Mortar (lump) from SU (Big Bath)
M202A	Bed mortar from SU 202, corresponding to a wall, side W (Big Bath)
M201B	Bed mortar from SU 201, external wall, WNW-ESE (Big Bath)
M171C	Bed mortar from SU 171, wall NNE-SSW (Big Bath)
M171E	Bed mortar from SU 171 wall NNE-SSW (Big Bath)
M171A_g	Bed mortar from SU 171 wall NNE-SSW (Big Bath)
M171A_b	Bed mortar from SU wall NNE-SSW (Big Bath)
M78C_g	Bed mortar from SU 78, external wall (Big Bath)
M78C_b	Bed mortar (lump) from SU 78, external wall (Big Bath)
M78C_b2	Bed mortar (lump) from SU 78, external wall (Big Bath)
M78A	Bed mortar from SU 78, external wall (Big Bath)
M78A_2n	Bed mortar from SU 78, external wall (Big Bath)
M78A_b	Bed mortar from SU 78, external wall (Big Bath)

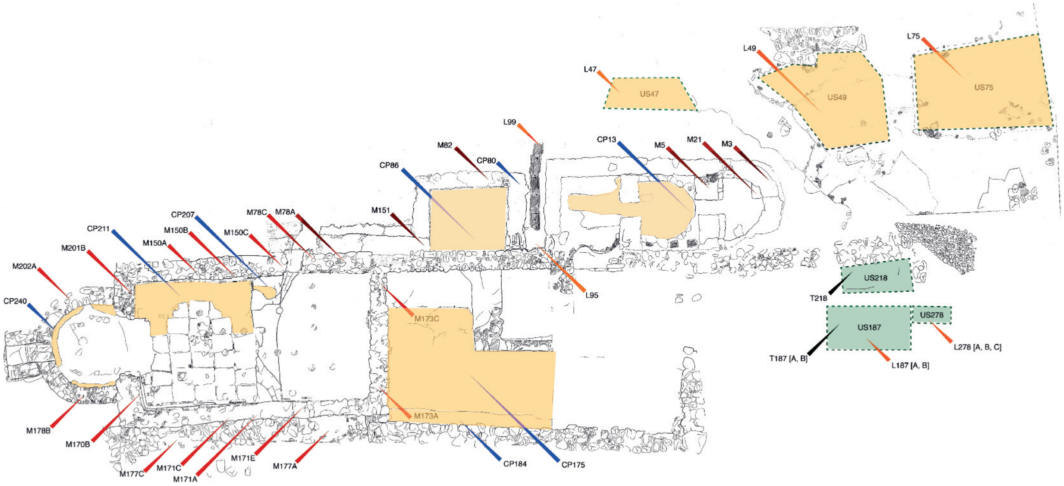

Figure 1. Scheme of the full-scale sampling in the Domo archaeological site. Red arrows indicate the sampling position of the 33 masonry mortars considered in this work (please note that multiple sampling has been done for some areas); blue, orange and black arrows indicate cocciopesto, brick and ground samples, respectively (not considered in this paper).

distance between the sample and the X-ray tube was 1.4 cm and the same applies for the distance between the sample and the detector. The working conditions are 25 kV and 0.3 mA with a 500 s acquisition time. The elements revealed for most samples were K, Ca, Mn, Fe, Cu, Zn and Sr. MDL values for trace elements were estimated considering background fluctuation and instrument sensitivity (de Vries, 1993) and were calculated to be between 40 and 50 ppm for Mn, Cu, Fe, Zn and 130 ppm for Sr due to the higher background in the spectral region.

XRD data (Cu-Kα, 1.5418 Å) were collected on a J-J Panalytical X'Pert PRO spectrometer. The diffractometer was equipped with a Ni filter and a solid state detector X'Celetator PW3015/20 diffractometer; the generator was operating at 40 kV and 40 mA. The diffractometer was also equipped with a linear Position Sensitive Detector (PSD), with the following optics: anti- scatter slit and divergence slit. The XRD scans were recorded from 3°-75° 2θ with 0.21°/sec and 5 min as total counting time for each scan. Grounded samples were placed in aluminium sample holder or dusted on frosted glass sample holder, depending on sample amount. In Table 2, relative intensities of minerals detected by XRD analysis for each sample are reported.

The preliminary observations made by stereo microscope allowed to schedule analysis in the best way and also to detect the presence of lumps in the mortar mixture and brown patina on some samples.

A good example of the presence of lumps is represented by the sample M150C: in this sample is evident a compact lump easily distinguishable from the surrounding mortar (Figure 2). Still characterized by the presence of lumps are samples M78C, M158B, M170B. It can be assumed that the lumps probably result from an incomplete or non optimal mixing procedure, which can mean a technique not too refined by manufacturers of the time. From the observations it was possible to see how the size of the aggregate change inside the samples: it goes from

Table 2. List of samples with relative intensities of minerals detected by XRD analysis. Different colours refer to different groups in HC analyses obtained by these data.

Samples	Quartz	Calcite	Fe and Mg carbonate	Aragonite	Clinochlore	Muscovite	Orthoclase	Plagioclase
M3	100	34			5	8	6	24
M5	100	36			6	10	5	18
M21	73	100			2	6	2	17
M78A	100	32			5	7	3	33
M78A_2n	100	29			3	12	7	18
M78A_b	100	32			5	7	3	33
M78C_b	2	100	3					
M78C_b2	8	100	2					
M78C_g	100	30			5	8	5	13
M82	100	64			5	10	5	22
M150A	100	17			4	7	4	25
M150B_b	30	100			1	3	2	6
M150B_g	100	42			10	25	7	27
M150C_b	3	100						
M150C_g	100	25			6	10	9	21
M151	100	63			6	12	7	14
M170B_b	7	100						
M170B_g	100	28			4	6	5	30
M171A_b	37	100						25
M171A_g	100	30			3	4	4	22
M171C	100	16			4	6	6	19
M171E	100	54			3	6	7	23
M173A_b	3	100		7				
M173A_g	100	45			7	14	11	30
M173C_b	14	100			1	3	1	5
M173C_g	100	23			4	5	4	20
M177A_b	40	100						1
M177A_g	100	83			2	4	3	15
M177C_b	4	100						
M177C_g	100	24			8	17	5	19
M178B	100	26			6	11	5	17
M201B	100	32			5	7	6	19
M202A	100	22			6	13	4	27

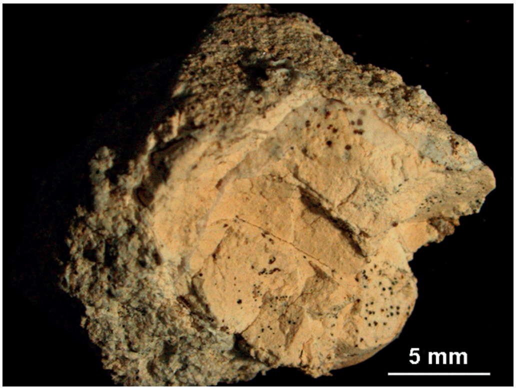

Figure 2. Stereo microscope shot of sample M150C: a compact lump, easily distinguishable from the surrounding mortar, is evident.

Figure 3. Stereo microscope shot of sample M150B: the size of the aggregate is few millimetres.

dimensions of a few millimetres as in the sample M150B, M171E and M201B (Figure 3), up to exceed largely the 5 mm as in M78C (Figure 4).

In addition it was possible to identify the presence of some brown-black areas on a few samples, namely M170B, M173C and M78A (Figure 5). X-ray fluorescence analysis results allow to identify them as patinas, probably of alteration, of iron and manganese.

As already said, the target of this work is to obtain a correct and rapid classification of the samples in order to get a sensible but limited sampling. So, using polychromatic radiation on light samples, the authors preferred not to perform quantitative analysis, but to work on the spectrum shape comparison. The entire ED-XRF spectra were submitted to multivariate analysis (Hierarchical Clustering) to get material classification thus basically comparing their shape and directly applying multivariate analysis on the acquired XRF spectra (Freitas, 2010; Calza, 2007). Three spectra - 4056 channels - were acquired for each sample and then averaged to lower background. Then, before undergoing

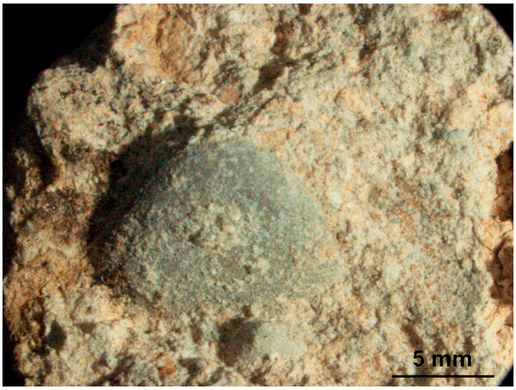

Figure 4. Stereo microscope shot of sample M78C: the size of the aggregate largely exceed 5 mm.

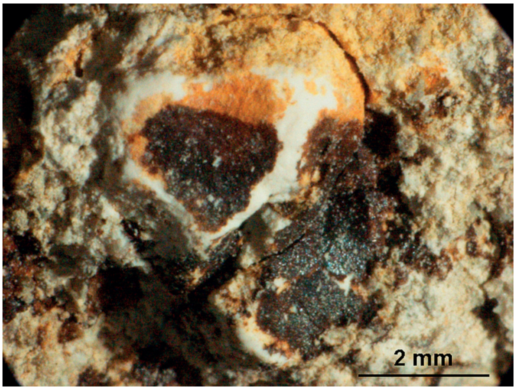

Figure 5. Stereo microscope shot of sample M170B: it is possible to see a brown-black area identified as a patina (iron and manganese detected by XRF analysis).

to HC, they have been smoothed (average on 2 nearest neighbors), normalised to coherent scattering peak and cut between 3 and 20 KeV (i.e. between K K_α and Mo K_α peaks). Then, as XRF peaks highly differ in intensity, logarithmic scale was used to make them comparable (Todeschini, 1998; Bonizzoni, 2013). Final plots were obtained by XLStat software on elaborated spectra.

XRD diffractograms were submitted to multivariate analysis in two different ways. The first try was to perform multivariate analysis of semi-quantitative proportional data (Table 2), but XRD diffractrograms are more complex than XRF spectra, so hierarchical analysis create fake groups, probably because of the inability to assess correctly the peaks with low intensity. Then to try to solve this problem and to ensure consistency with the XRF analysis, the same statistic treatment on entire diffractrograms was applied. The colour in Table 2 are referred to the grouping obtained (see below) by Hierachical Clustering analysis; the number in the names refers instead to the Stratigraphic Unit. As for XRF analysis, XRD diffractograms were submitted to Hierarchical Clustering analysis using a logarithmic scale to prevent too high differences in peak intensity between primary and secondary compounds.

In both cases dendrograms were created exploiting Euclidean distance and Ward's linkage method that minimize the Sum of Squares of any two (hypothetical) clusters that can be formed at each step (Zhu, 2004).

Data analysis and results

Dendrogram obtained from the 33 acquired XRD diffractograms and XRF spectra on ground samples are shown in Figures 6 and 8, respectively.

Considering XRD diffractogram results, the main difference between the two biggest groups (named AD and BD) is the intensity of the peaks of quartz and calcite. The first two clusters (highlighted in blue and named AD1 and AD2 respectively) group samples that show more intense peaks of quartz compared to the ones of calcite. All these spectra show in addition the presence of chlorite, muscovite, plagioclase and orthoclase: all these minerals, together with quartz, are typical of sand, which is added to lime to produce mortar. The samples in the first group (AD1 group) show instead low peaks of calcite and intense peaks of orthoclase, as well as the presence of the other secondary minerals. On the opposite, the second group (AD2 group) is characterised by very low peaks of calcite and intense peaks of chlorite and muscovite, beside the presence of minor minerals. On the other hand, the big red group (indicated as BD) shows more intense peaks of calcite, whereas the ones of quartz are lower, and a very low, or even absence, presence of secondary minerals.

Figure 7 shows the comparison between XRD spectra from two samples (namely M150C_b and M150A), pertaining to the two cluster described above. The two smaller sub-clusters (highlighted in yellow and orange, respectively) are exclusively due to the difference in the signal/noise ratio of the spectra acquired.

The dendrogram obtained from XRF spectra analysis shows clearly two groups: samples pertaining to the first group, the blue one (named AF), and to the second group, the red one (BF), are the same of corresponding groups for XRD results. Both groups are characterised mainly by the presence of Ca and Fe, as well as other secondary elements; the clustering derives mainly from different relative concentration of these two elements: the blue group are richer in Fe than in Ca, instead the red one has peaks of Ca more intense than the ones of Fe.

This corresponding is highly encouraging because it allows to discriminate between the two main type of mortar present in this site with a rapid and in situ non destructive XRF measuring campaign. In Figure 9 a comparison between XRF spectra from sample M150C_b

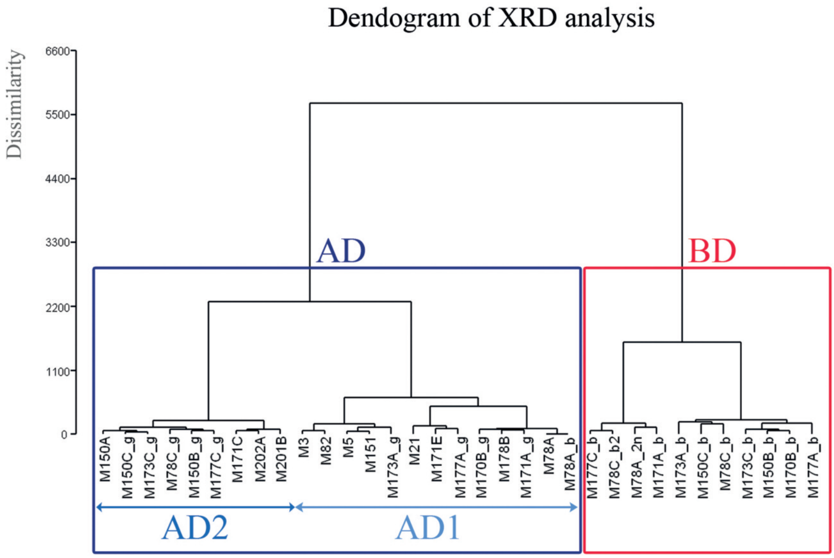

Figure 6. Dendogram from XRD diffractogram analysis. For clusters description see in the text.

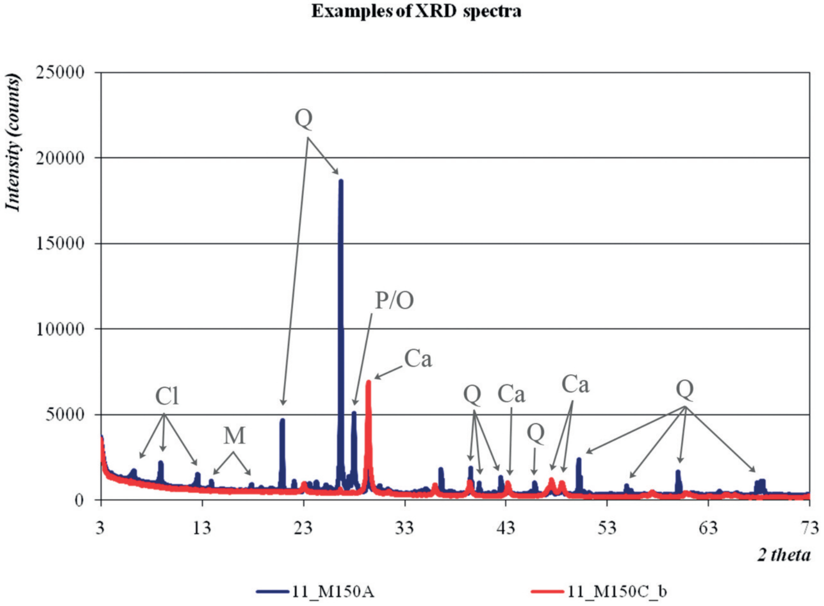

Figure 7. Comparison between XRD diffractograms of sample M150A and M150C_b. Diffractogram colours are referred to belonging cluster. Only principal peaks are specified (Ca = Calcite, Cl = Chlorite, Q = Quartz, M = Muscovite, P/O = Plagioclase or Orthoclase).

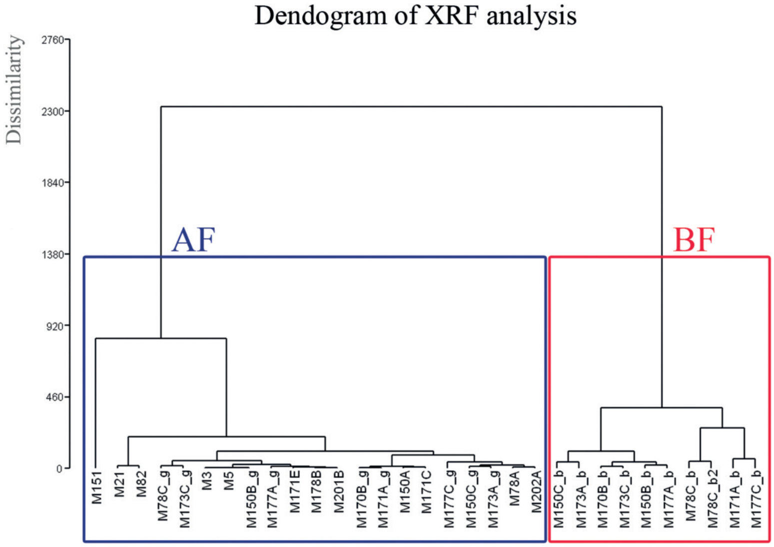

Figure 8. Dendogram from XRF spectra analysis. For clusters description see in the text.

(red group) and M150A (blue group) is reported as an example.

From the data reported in Table 2, it is clear than none of the secondary mineral revealed contains iron, well detected in the XRF spectra, as evident in the spectra reported in Figure 9. As general remark, we must remember that minimum detection limits for metals in XRF is much higher than those for minerals in XRD. Moreover, detection efficiency for Ca is much lower than for Fe. This means than XRF can detect iron also when it is present in minerals with too low concentration for XRD detection. On the other hand, ED-XRF portable spectrometer can detect chemical elements with atomic number above 18; so, Si, Al and Mg, for instance, are not detected even if present in high concentration. This gives a complementary point of view from XRD and XRF analyses. It is very interesting to note that these independent analytical techniques bring the same grouping on different basis; this means that minority minerals from XRD are associated to other minerals which are possible present in a very low concentration, under 1%. Nonetheless, chemical elements characterising these minerals can be detected by XRF.

Conclusions and outlooks

Multivariate analysis was performed both on the spectra obtained by XRF and on XRD diffractograms. The comparison between the groups obtained by results of the two analytical techniques clearly show how both analyses lead to create two macroclusters characterised by the greater presence of quartz (blue groups) or calcite (red groups) for the XRD analysis, and for a different level of reciprocal concentration of iron and calcium for XRF analysis. This two aspects show the great advantages to use several independent analytical techniques to get a more complete information. The elemental analysis may therefore be useful in case it is necessary to execute a first evaluation, directly in situ and for a subsequent sampling of the mortars to be subjected

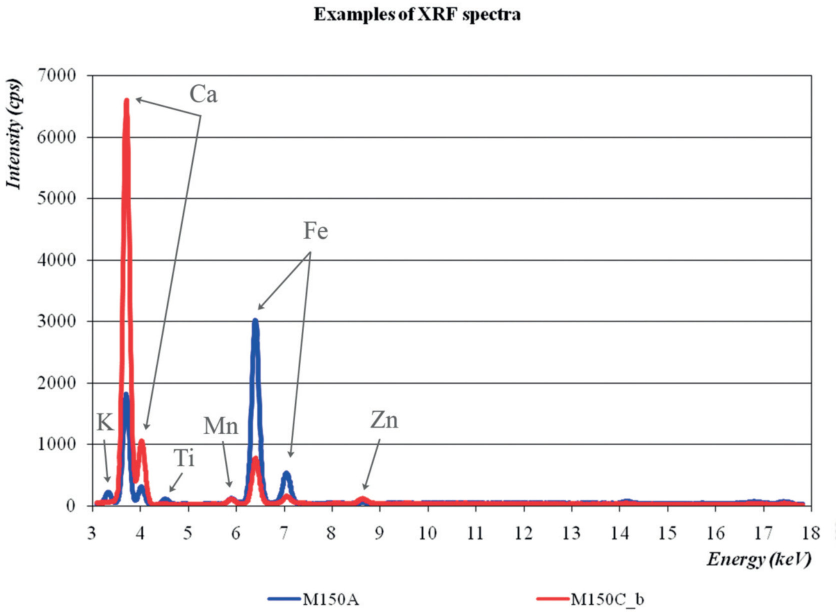

Figure 9. Comparison between XRF spectra of sample M150A and M150C_b. spectra colour are referred to belonging cluster. Only principal peaks are specified.

to further analysis, such as diffractometry. In our case, XRD measurements have produced two additional meaningful sub-clusters in the big blue one, characterised by a different relative concentration of secondary minerals. In the next archaeological campaign, XRF analysis on site on untreated samples will be applied to verify the real possibility on discriminating on line the two groups detected. Then, an advised sampling will select a few samples for chemical laboratory analyses to ensure the accuracy of the results. Compositional characterization of ceramics is also foreseen, together with termoluminescence (TL) dating. Considering works now in progress, also OSL dating of the mortar samples will be of great help (Goedicke, 2011; Panzeri, 2013). This large scale investigation should allow to get extended information about building materials and to compare them with the archaeological hypothesis. This will actually help to reconstruct the steps of use and the changes that occurred in time to the bath complex and that are no longer directly deducible from archaeological practice, clarifying, controverting or suggesting archaeological interpretation.

The archaeological feedback are currently in progress: the groups generated by the analysis will be compared with the stratigraphic hypothesis to reconstruct the phases of use and the changes that occurred in time to the bath complex. At a preliminary observation, the analyses show that probably the builders used the same raw material for the bath complex although it was built in different times and even if some features in the materials were found corresponding to anthropic actions aimed at changing the intended use of the structures. Only the results of the forthcoming excavations will be able to confirm or deny these preliminary interpretations.

Ackwnoledgements

The authors would like to thank for their collaboration: Lorenzo dell'Aquila, Archeodomani sas, and Alfredo Guarino for the coordination and scientific direction of the archaeological excavation that took place in Bibbiena (AR); Claudia Conti e Marco Realini for mineralogical analysis carried out at ICVBC-CNR.

Two anonymous referees are thanked for their help in improving the manuscript.

References

Adam J.P. (1989) - L'arte di cosruire presso i romani, materiali e tecniche, Ed. Longanesi & C.

Aranguren B.M., Brocchi L., Lari D., Ducci M. and Fedeli L. (1999) - Gruppo Archeologico Casentinese G.A.C., Comunità montana del casentino, Il Casentino dalla Preistoria al Medioevo, Profilo di una valle attraverso l'archeologia.

Bonizzoni L., Galli A., Gondola M. and Martini M. (2013) - Comparison between XRF, TXRF and PXRF analyses for provenance classification of archaeological bricks. *X-Ray Spectrometry*, 2013, 42, 262-267.

Calza C., Anjos M.J., Bueno M.I.M.S., Mendonça de Souza S., Brancaglion A.Jr, Lima T.A. and Lopes R.T. (2007) - XRF applications in archaeometry: analysis of Marajoara pubic covers and pigments from the sarcophagus cartonage of an Egyptian mummy. *X-Ray Spectrometry,* 36, 348-354.

De Vries J.L. and Vrebos B.A.R. (1993) - In: Handbook of X-ray Spectrometry. Methods and Techniques. (eds): R.E. Van Grieken and A.A. Markowic, Marcel Dekker, Inc., New York.

Freitas R.P., Calza C., Lima T.A., Rabello A. and Lopes R.T. (2010) - EDXRF and multivariate statistical analysis of fragments fromMarajoara ceramics. *X-Ray Spectrometry*, 39, 307-310.

Goedicke C. (2011) - Dating mortar by optically stimulated luminescence: a feasibility study. *Geochronometria*, 38, 42-49.

Panzeri L. (2013) - Mortar and surface dating with Optically Stimulated Luminescence (OSL): Innovative techniques for the age determination of buildings. *Il nuovo Cimento C*, 36, 205-216.

Tite M.S. (2008) - Ceramics production, provenance, use - a review. *Archaeometry*, 50, 216-231.

Todeschini R. (1998) - Introduzione alla Chemiometria, EdiSES: Napoli.

Zhu J., Shan J., Qiu P., Qin Y., Wang C., He D., Sun B. and Tong P. (2004) - Wu S. The multivariate statistical analysis and XRD analysis of pottery at Xigongqiao site. *Journal of Archaeological Science*, 31, 1685-1691.

Submitted, May 2013 - Accepted, November 2013